Hot Deformation and Dynamic Recrystallization of the Beta Phase in Titanium Alloys

Frank Montheillet, Lois Pallot, David Piot

Hot Deformation and Dynamic Recrystallization of the Beta Phase in Titanium Alloys

F. Montheillet[1, a], L. Pallot[1,2,b] and D. Piot[1,c]

[1]Ecole des Mines de Saint-Etienne (Centre SMS), CNRS UMR 5146, 158 cours Fauriel, 42023 Saint-Etienne Cedex 2, France

[2]Snecma Gennevilliers, département Qualité, Matériaux et Procédés, 171 bd. de Valmy, BP 31, 92702 Colombes Cedex, France

[a]montheil@emse.fr (corresponding author), [b]pallot@emse.fr, [c]piot@emse.fr

Keywords: hot working, titanium, recrystallization, modeling

Abstract Due to the high rate of dynamic recovery associated with the large stacking fault energy of the bcc structure, classical "discontinuous" dynamic recrystallization, occurring by nucleation and growth of new grains is not observed in the β phase of titanium alloys. Instead, the following mechanisms take place: at low and moderate strains ($\varepsilon < 1$), the original flattened (compression) or sheared (torsion) grains are still recognizable, although their boundaries are strongly serrated. In this strain range, grain size (thickness) results from both the convection and the migration of grain boundaries. At intermediate strains, "geometric" dynamic recrystallization leading to "pinching off" events of the original grains is observed, whereas at larger strains ($\varepsilon > 5$), grain fragmentation occurs by the generation of new grain boundaries ("continuous" dynamic recrystallization). The associated flow stress often exhibits pronounced softening and the resulting (equiaxed) grain size can be much smaller than the initial one. It is worth to note that a very similar sequence of mechanisms takes place in ferritic steels, as well as in aluminium alloys, in spite of their different crystallographic structure. In this paper, the above mechanisms will be illustrated by a set of data pertaining to titanium alloys.

Introduction

Thermomechanical processing of titanium alloys used for aeronautical applications involves quite complex forging schedules. In most cases, such alloys display a single bcc β phase domain at higher temperatures, whilst below the transus temperature θ_β the material is made of an aggregate of hcp α and bcc β phase. Since the flow stress of α is much larger than that of β, the overall flow stress strongly increases with decreasing temperature under the combined effects of thermal activation associated with the two individual phases and the rapid increase of the α fraction when temperature lowers [1]. It is necessary, however, to strain the material within the two phase range, in order to break the lamellar microstructure inherited by cooling from the β range. The forging schedules must therefore be carefully tailored to account for this requirement without exceeding the load capacities of the tools. An example of such schedule is shown in Fig. 1.

The β to α phase transformation occurring upon cooling after a forging step in the β range, as well as the resulting microstructures, obviously depend on the hot deformation mechanisms which take place during β forging. The latter can be directly investigated in the β-metastable alloys, such as *Ti-17*, Ti-10-2-3, Ti-555-3, or *Betacez*, after quenching the deformed microstructures. Due to the high rate of dynamic recovery associated with the large stacking fault energy of the bcc structure, classical "discontinuous" dynamic recrystallization, occurring by nucleation and growth of new grains is not observed. Instead, various mechanisms take place, which will be reviewed in this paper. In fact, experimental data show that the hot deformation behaviour of the β phase in titanium alloys is quite similar in ferritic steels or the bcc α phase of standard steels, as well as in aluminium alloys, in spite of their different crystallographic structures, which will be illustrated by some examples. Finally, models formerly proposed for these mechanisms will be briefly reminded.

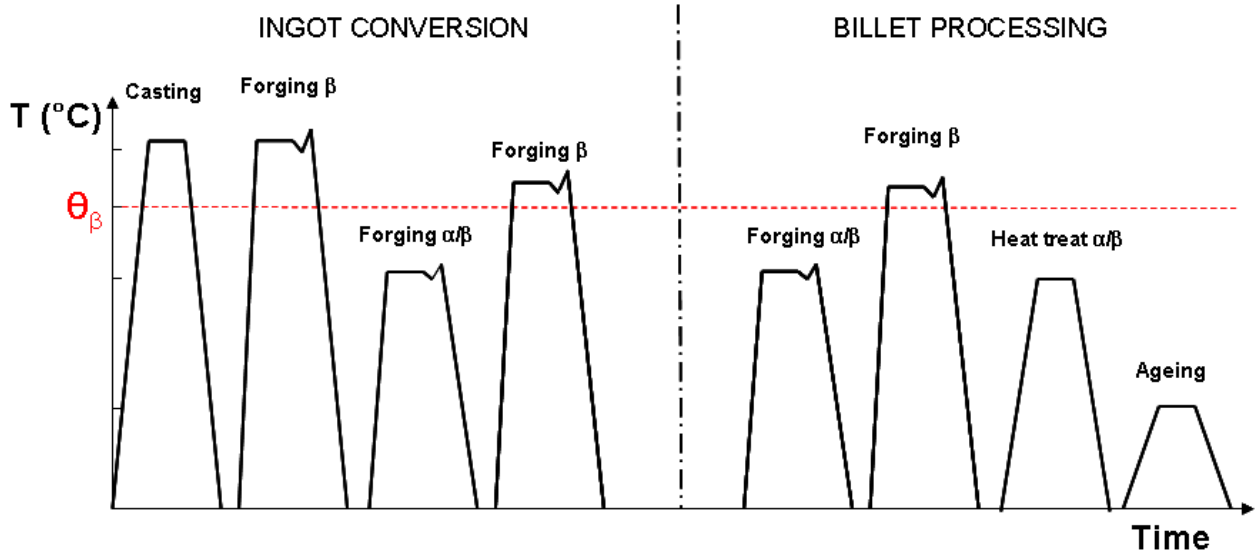

Figure 1. Example of a forging schedule for the alloy Ti-17. The left part of the drawing corresponds to the ingot conversion; the right part is associated with the transformation of the billet into a workpiece. Three forging steps are carried out within the β phase

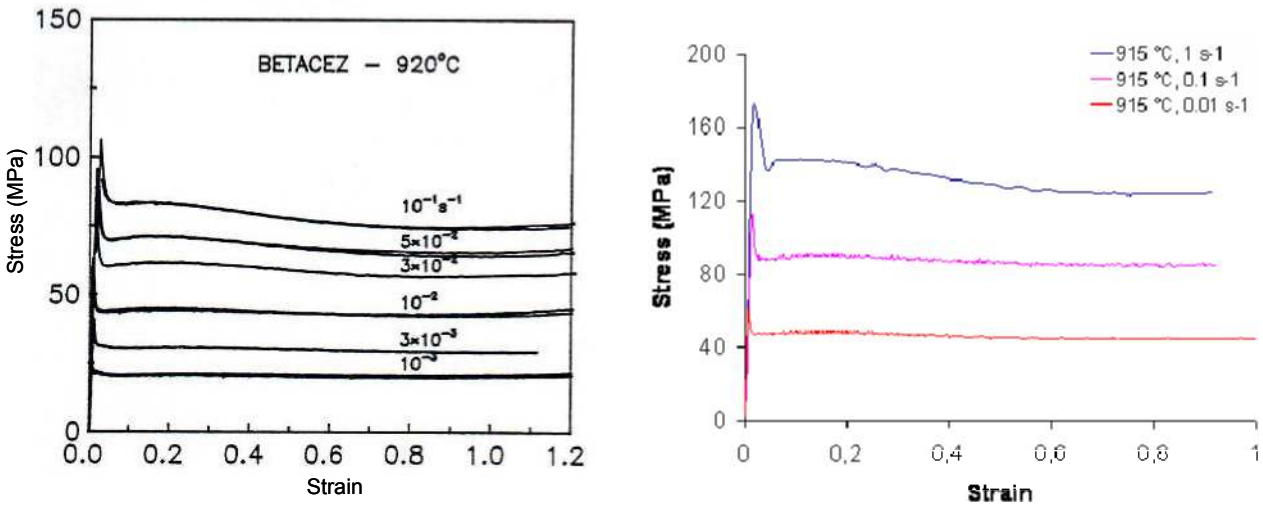

(a) (b)

Figure 2. Examples of stress-strain curves pertaining to the *Betacez* [2] (a) and *Ti-17* [3] (b) alloys in the β domain (uniaxial compression tests at constant strain rates)

Stress-strain curves

It is first interesting to glance at the flow stress behaviour of the β phase, before investigating the deformation mechanisms. Figs. 2a and b show stress-strain curves obtained from uniaxial compression tests on *Betacez* at 920 °C ($\theta_\beta \approx 890$ °C) and Ti-17 at 915 °C ($\theta_\beta \approx 890$ °C), respectively, carried out over the same range of constant strain rates. After an initial peak, which is more pronounced at larger strain rates, the flow stress decreases smoothly to reach some apparently steady value. However, when very large strains are prescribed, the torsion results reported in Fig. 3 show that the "true" steady state is only attained after an equivalent strain of 5 or more. Moreover, a

considerable softening is observed at 0.1 and 1 s^{-1}. The latter has not yet been definitively explained, although it may be partly ascribed to self-heating, texture formation, or continuous dynamic recrystallization (see below).

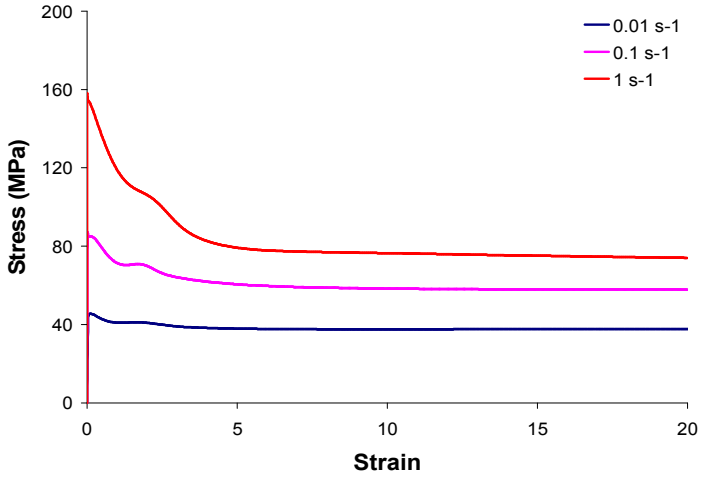

Figure 3. Torsion stress-strain curves of *Ti-17* specimens up to an equivalent strain of 20 [3]

Microstructural changes during deformation

Although the various mechanisms involved overlap upon increasing strain, it is convenient to distinguish three domains associated with low and moderate strains ($\varepsilon < 1$), intermediate strains, and large strains ($\varepsilon > 5$), respectively.

At low to moderate strains, the original flattened (compression) or sheared (torsion) grains are still recognizable, although their boundaries are strongly serrated. Grain size, or rather grain thickness, is determined by the combination of convection and migration of the grain boundaries [4]. Under uniaxial or plane strain compression, the average grain thickness measured parallel to the compression axis decreases during straining. Applying to a first approximation the uniform strain (Taylor) assumption, this leads to the merely geometrical prediction:

$$H = H_0 \exp(-\varepsilon) \quad (1)$$

where H and H_0 denote the current and initial grain thicknesses, respectively, and ε is the logarithmic strain of the specimen. However, a number of metallographic investigations carried out on β titanium alloys and an aluminium alloy have shown that the measured average thickness H_{exp} is systematically larger than H [4]. Moreover, it tends to an asymptotic value instead of steadily decreasing as predicted by Eq. 1. This can be attributed to dynamic grain growth occurring during hot deformation, which opposes the geometrical effect accounted for by Eq. 1. A simple average grain model leads to the modified equation [4]:

$$H = H_s - (H_s - H_0)\exp(-\varepsilon) \quad (2)$$

where $H_s = 2v_{app}/\dot{\varepsilon}$ is the asymptotic steady state value of H, v_{app} the average migration rate, and $\dot{\varepsilon}$ the prescribed strain rate. From the above equation and appropriate metallographic measurements, it is easy to determine v_{app}. Nevertheless, this approach is too simplified, since only a part of migrating boundaries participate to grain growth, while the thickness of some grains currently decreases or remains constant. In fact the true origin of average grain growth is the disappearance of grains when boundaries impinge together. Such effects have been taken into account in a one-dimensional numerical model considering a "stack" of grains in [4]. A conclusion was that there is an almost linear relationship between the average "true" migration rate v_m and the apparent one v_{app}:

$$v_m \approx 2\, v_{app} \qquad (3)$$

With this approach, the migration rate of grain boundaries *during hot deformation* can therefore be readily estimated. Values close to 1 µm/s have been recently obtained in this way for the alloy Ti-17 strained at 915 or 945 °C and 0.01 s^{-1}.

At intermediate strains, grains become strongly serrated in association with the generation of a large number of subgrain boundaries. The "wavelength" of the serrations strongly decreases with increasing strain rate, since it is approximately equal to the subgrain size, which itself varies linearly with the reciprocal of the flow stress (Figs. 4a and b). This mechanism leads to "geometric" dynamic recrystallization, *i.e.* the local "pinching off" and fragmentation of the elongated and flattened original grains. Although this mechanism has been proposed a long time ago, only a few attempts of mathematical modeling are available to date [5]. Moreover, at larger strain rates, whereas the migration rate is likely to be larger due to stronger driving forces, it is counterbalanced by the reduction of the migration time, which results in much smaller boundary migration distances. The overall result is a much lower efficiency of geometric dynamic recrystallization, as illustrated in Fig. 4b.

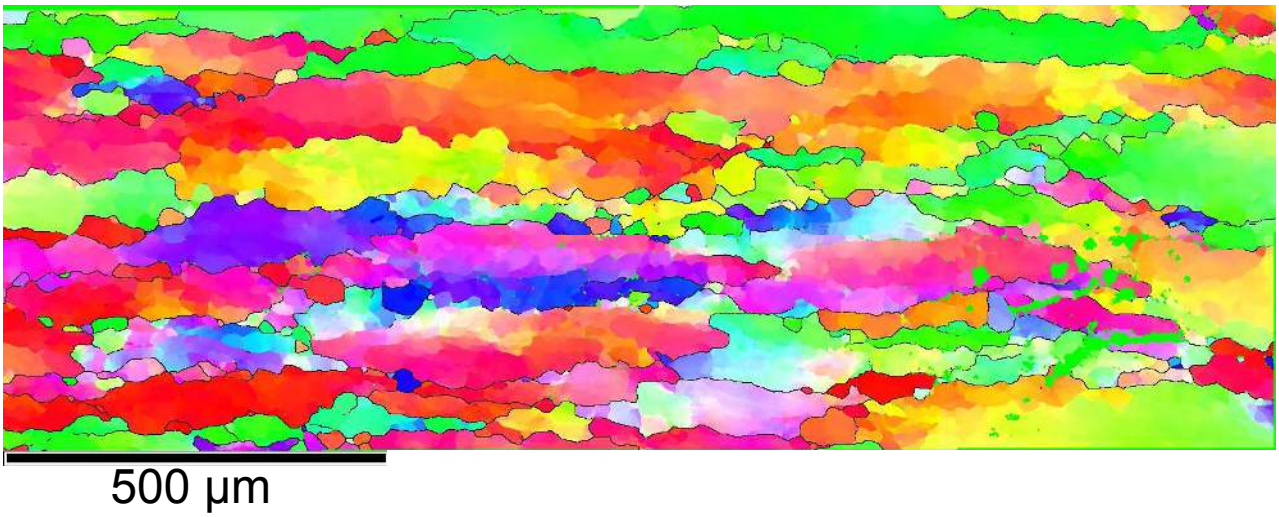

(a) 915 °C, $\varepsilon = 1$, $\dot{\varepsilon} = 0.01\ s^{-1}$

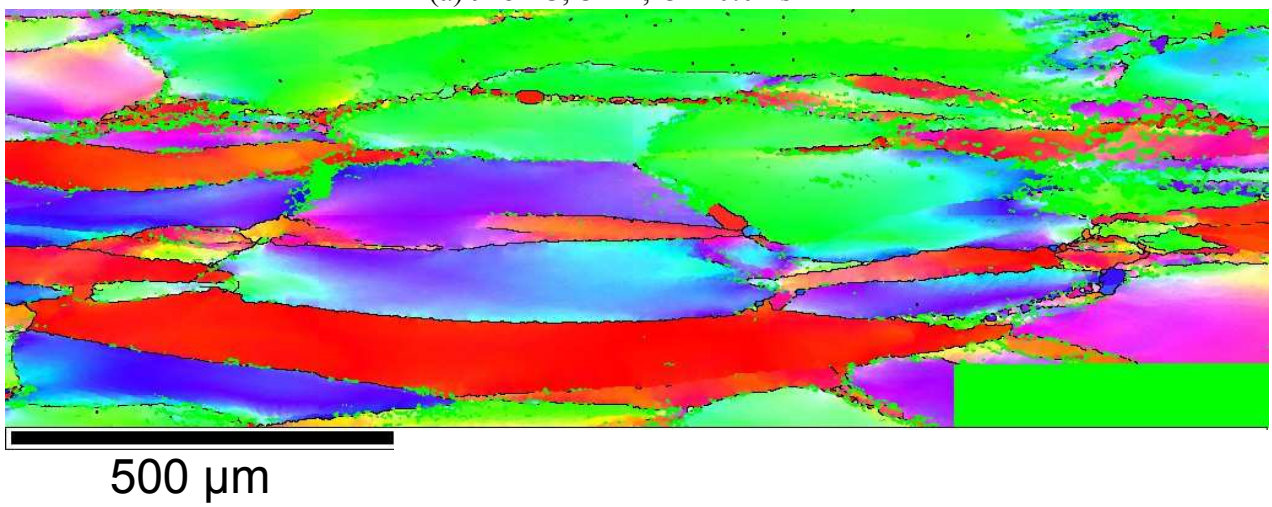

(b) 915 °C, $\varepsilon = 1$, $\dot{\varepsilon} = 1\ s^{-1}$

Figure 4. EBSD maps showing hot compression microstructures of alloy *Ti-17*. Colors indicate the crystallographic orientations of the compression axis (vertical in the figure) (red: <100>, green: <110>, blue: <111>) [3]

At large strains, achieved by torsion testing, initial grains are completely fragmented and cannot yet be recognized. A steady state microstructure is obtained, the parameters of which are independent of the initial grain size of the material. An example is shown in Fig. 5 in the case of alloy *Ti-17* strained to $\varepsilon = 14$ (EBDS map). The same microstructure is displayed in Fig. 6a, where the high angle (HAB) and low angle (LAB) boundaries are highlighted by two different colours. It appears clearly that high angle boundaries do not systematically close up around grains, like in a classical statically recrystallized material. Such microstructure has therefore been termed as made of crystallites rather than grains and subgrains. Fig. 6b exhibits similar characteristics in a ferritic stainless steel strained to $\varepsilon = 20$ at 800 °C and 1 s^{-1}. Note, however, that the Zener-Hollomon parameter was significantly larger in this case, ($Z \approx 1.1 \times 10^{11}$ s^{-1} instead of 5.3×10^{4} s^{-1}) leading to a much finer crystallite microstructure.

In low stacking fault energy materials (*e.g.*, copper, austenitic steels), "discontinuous" dynamic recrystallization (DDRX) occurs, since large local concentrations of elastic energy lead to the nucleation of new grains during deformation. Quite fast boundary migration rates prevent any transformation of low angle boundaries into large angle boundaries. By contrast, in high stacking fault energy metals (*e.g.*, aluminium, ferritic steels, β phase of titanium or zirconium alloys), the strong effect of dynamic recovery impedes nucleation of new grains, thus allowing the generation of new grain boundaries by progressive misorientation of low angle boundaries. This mechanism, referred to as "continuous" dynamic recrystallization (CDRX) has not yet been extensively investigated, especially at large strains. A simple physically based model has nevertheless been proposed, where the crystallite microstructure is represented schematically in Fig. 7. Flow stress levels and steady state crystallite sizes, as well as subgrain boundary misorientation distributions have been correctly predicted by this model [7].

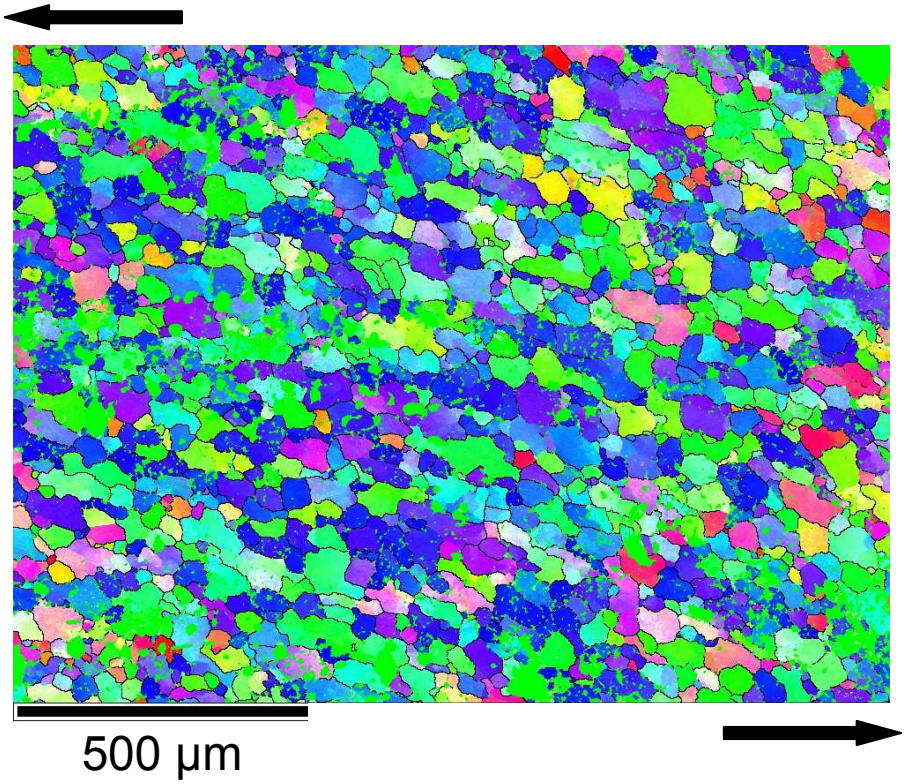

Figure 5. Large strain hot torsion microstructures of alloy *Ti-17*. 915 °C, $\dot{\varepsilon} = 0.01$ s^{-1}, $\varepsilon = 14$. Colors indicate the crystallographic orientations of the shear axis (arrows) (red: <100>, green: <110>, blue: <111>) [3]

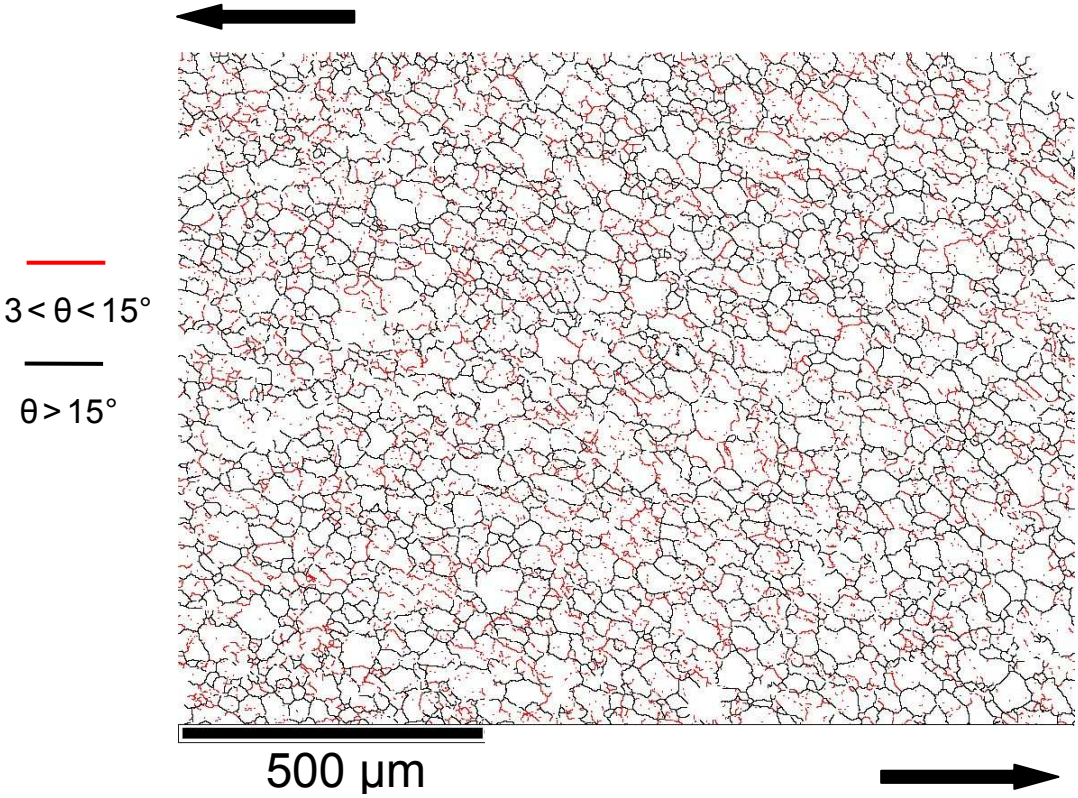

(a) alloy *Ti-17*, 915 °C, $\dot{\varepsilon} = 0.01\ s^{-1}$, $\varepsilon = 14$ ($Z \approx 5.3 \times 10^4\ s^{-1}$)

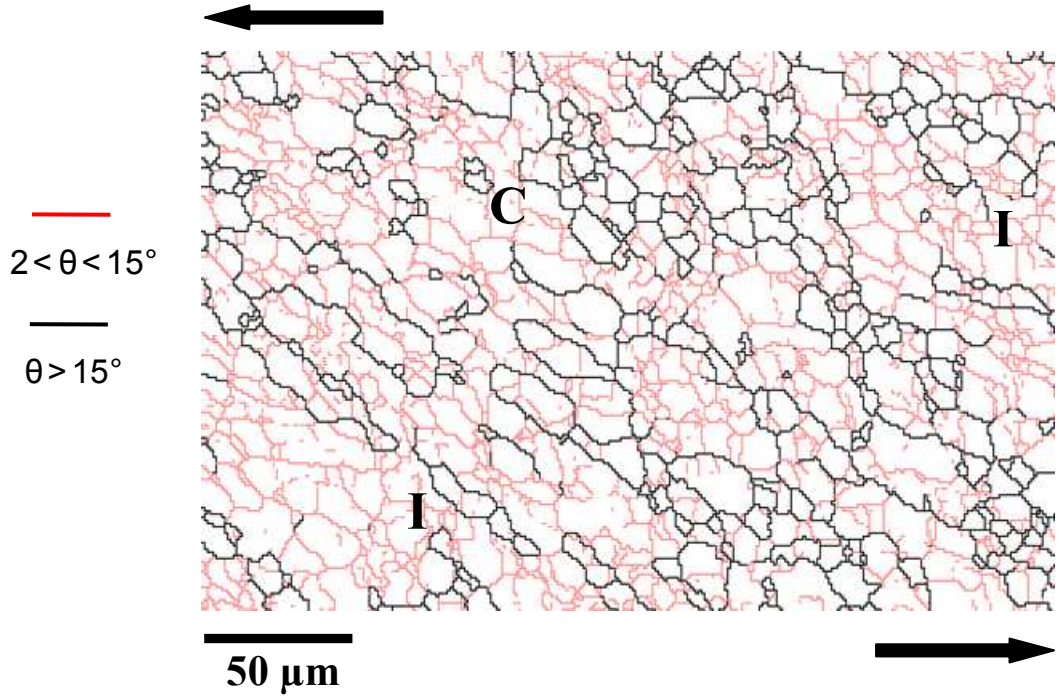

(b) Ferritic 11 %Cr stainless steel, 800 °C, $\dot{\varepsilon} = 1\ s^{-1}$, $\varepsilon = 20$ ($Z \approx 1.1 \times 10^{11}\ s^{-1}$) [6]

Figure 6. Large strain hot torsion microstructures of two bcc materials (EBSD boundary maps). C and I denote closed and isolated grain boundaries, respectively.

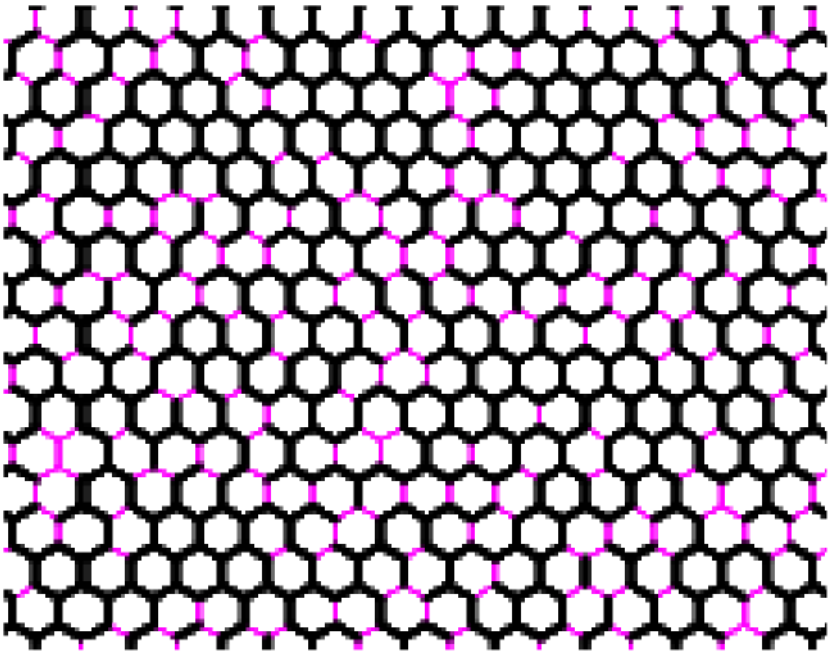

Figure 7. Schematic representation of a crystallite microstructure involving crystallites surrounded by high angle boundaries (black) and low angle boundaries (pink).
Here $f_{HAB} = 0.75$ and $f_{LAB} = 0.25$

Summary

In this short overview, it has been underlined that microstructural changes occurring during hot deformation of titanium alloys in the β range can be decomposed into three strain domains involving (i) deformation of the initial grains, (ii) generation of some new grains by geometric dynamic recrystallization, and (iii) complete fragmentation of the original microstructure by continuous dynamic recrystallization (generation of new high angle boundaries). Furthermore, a very similar sequence of overlapping mechanisms is observed in ferritic steels and aluminium alloys.

References

[1] L. Briottet, J.J. Jonas and F. Montheillet, A mechanical interpretation of the activation energy of high temperature deformation in two phase materials, Acta Metall. Mater. 44 (1996) 1665-1672.

[2] F. Montheillet, D. Dajno, N. Come, E. Gautier, A. Simon, P. Audrerie, A.-M. Chaze and Ch. Levaillant, Hot deformation of the new high strength *Betacez* titanium alloy, 7th World Conference on Titanium (Titanium '92), San Diego (1992), pp. 1347-1354, The Minerals, Metals and Materials Society (1993).

[3] L. Pallot, D. Piot, C. Desrayaud, F. Montheillet and A. Bénéteau, Traitement thermomécanique de l'alliage Ti-17 dans le domaine bêta. Matériaux 2010, Nantes, DVD publication (2010).

[4] S. Gourdet and F. Montheillet, Effects of dynamic grain boundary migration during the hot compression of high stacking fault energy metals. Acta Mater. 50 (2002) 2801-2812.

[5] L. De Pari Jr. and W.Z. Misiolek, Theoretical predictions and experimental verification of surface grain structure evolution for AA6061 during hot rolling, Acta Mater. 56 (2008) 6174-6185.

[6] T. Reis de Oliveira. Effet du niobium et du titane sur la recristallisation dynamique d'aciers inoxydables ferritiques stabilisés, PhD Thesis, Ecole des Mines de Saint-Etienne, France (2003).

[7] S. Gourdet et F. Montheillet, A model of continuous dynamic recrystallization, Acta Mater. 51 (2003) 2685-2699.